Journal of The Electrochemical Society, **158** (3) G52-G57 (2011)
0013-4651/2011/158(3)/G52/6/$28.00 © The Electrochemical Society

Effect of Curing on the Porogen Size in the Low-*k* MSQ/SBS Hybrid Films

Yu-Han Chen,[a] U-Ser Jeng,[b] and Jihperng Leu[a,*,z]

[a]*Department of Materials Science and Engineering, National Chiao Tung University, Hsinchu 300, Taiwan*
[b]*National Synchrotron Radiation Research Center, Hsinchu 300, Taiwan*

The interaction between a polystyrene-*b*-polybutadiene-*b*-polystyrene (SBS) porogen and a low-*k* methylsilsesquioxane (MSQ) matrix under different curing profiles and their impact on porogen size were studied by grazing incidence small-angle X-ray scattering, viscosity measurement, and Fourier transform infrared analysis. For slow curing, significant porogen diffusion and aggregation occurred between 100 and 170°C, at which the porogen size increased from 12 to 32 nm. The interaction mechanism between porogen and the MSQ matrix and its correlation with porogen size during the thermal cure process were elucidated. The aggregation of the SBS porogen was greatly influenced by the microstructure of the MSQ matrix at three controlling temperatures; namely, (1) glass transition temperature, T_g (~ 100°C), (2) onset temperature (160°C) for transforming cage to network structure, and (3) immobilization temperature (170°C). In contrast, a rapid curing rate enabled the formation of small porogen size (~ 12 nm) in the hybrid films and yielded better mechanical strength.
 [DOI: 10.1149/1.3529246]

Manuscript submitted June 22, 2010; revised manuscript received November 18, 2010. Published January 13, 2011.

As the feature size of microelectronic devices continues scaling down, the increase in resistance-capacitance (RC) delay, cross talk noise, and power dissipation in the interconnect structure become the limiting factors in the ultra-large-scale integration of integrated circuits.[1] To further reduce the delay, materials with low dielectric constants (low-*k*) ranging from 2.65 to 3.0 were introduced to reduce the parasitic capacitance 28–37% less than that of SiO_2 (k = 4.2) and 19–28% less than that of fluorosilicate glass (k = 3.7).[2] Moving further toward a 45 nm node and beyond, the incorporation of porosity, in which air has k_{air} = 1, the lowest attainable value,[3] becomes essential for producing viable low-*k* materials with $k < 2.5$.[4] Conventionally, porous low-*k* dielectric films are generally formed following the deposition of a low-*k* matrix with a thermally liable pore generator (porogen)[5] such as norbornene-derivative,[6] polyoxyethylene ether,[7] and amphiphilic block copolymers (ABCs), including poly(ethylene oxide-*b*-propylene oxide-*b*-ethylene oxide)[8,9] and poly(methyl methacrylate-co-dimethylaminoethyl methacrylate),[10,11] which are burned out by thermal treatment at low temperatures, typically ≤200°C immediately following the deposition of the film.

However, various problems associated with the integration of as-deposited porous dielectrics have been identified.[12,13] These include (1) high leakage and device reliability at the barrier/low-*k* interface because of insufficient coverage for large pores,[12] and (2) large variation in RC delay caused by the significant roughness in the dielectric due to etching.[13] To solve these problems, a postintegration porogen removal scheme[14] based on material design and process integration has been proposed. It employs high-temperature porogen to defer the formation of a porous low-*k* dielectric until the completion of the copper chemical-mechanical polishing (CMP) step, and then thermally removes the sacrificial porogen from the hybrid dielectric film, as illustrated in Fig. 1. In the postintegration porogen removal scheme, the porogen in the hybrid low-*k* matrix/porogen films must survive at the highest possible processing temperature (preferably 300–350°C) cycling of back-end-of-line processing steps. Accordingly, the decomposition temperature (T_d) of high-temperature porogen candidates must exceed 350°C to implement the postintegration porogen scheme. Polystyrene-*b*-polybutadiene-*b*-polystyrene (SBS) with $T_d > 350$°C is a favorable candidate porogen because of its thermal stability. In addition, its amphiphilic characteristics can significantly improve the miscibility of the MSQ/porogen hybrid, which prevents phase separation prior to the burning out step.[8,9]

For such hybrid films to survive the backend processing such as the CMP step in the postintegration porogen removal scheme, the hybrid low-*k* material should possess sufficiently strong mechanical strength. Moreover, the mechanical property, such as Young's modulus of the hybrid films, depends on the porogen morphology, size, and size distribution, among other factors, including, for instance, the chemical structures of the matrix and degree of cross-linking. Yet, the interaction between the porogen and low-*k* matrix during curing and their impact on the porogen size of low-*k*/porogen hybrid films are not fully understood. Thus, it is of critical interest to understand the porogen behavior and how to control its size in the low-*k* matrix/porogen hybrid films before burning out porogen to form a porous low-*k* film.

In this paper, a commercial, spin-on organosilicate, i.e., methylsilsesquioxane (MSQ) was selected as the matrix and a high-temperature porogen such as SBS, was employed as the sacrificial component. The effects of the curing rate (slow, 2°C/min vs rapid, 200°C/min) and cure temperature on the porogen size in the hybrid low-*k* films cured up to 200°C were studied by in situ grazing incidence small-angle X-ray scattering (GISAXS), viscosity measurement, and Fourier transform infrared (FTIR) analysis. The impact of the MSQ structure during the thermal cure process on the porogen aggregation behavior and its correlation with porogen size will be described and elucidated.

Experimental

The low-dielectric-constant matrix, MSQ, was obtained from Gelest, Inc. MSQ has two main structures; namely, a cage structure and a network structure.[15,16] Polystyrene-block-polybutadiene-block-polystyrene (28% polystyrene Mw = 90,000 g/mole) triblock copolymer, as the high-decomposition-temperature porogen (T_d ~ 390°C), was obtained from Sigma-Aldrich Co. To form hybrid low-*k* films, MSQ and SBS at 5 wt % loading were dissolved in tetrahydrofuran (THF) to form a hybrid low-*k* solution without special treatment such as surfactants to further minimize the porogen size. The solution was initially filtered through a 0.20 μm PTFE filter (Millipore, Inc.), and then spun onto a (100) silicon wafer at 2000 rpm for 30 s at room temperature to obtain a film thickness of 500 nm.

The sizes of the porogen in the hybrid low-*k* films were then characterized by in situ GISAXS under two curing profiles: (1) slow curing at 2°C/min and (2) rapid curing at approximately 200°C/min. In situ 2D GISAXS data were collected from 30 to 210°C in intervals of 20°C, in which data collection times are 5 and 2 s for slow and rapid curing profiles, using beamline 17B3 of the National Synchrotron Radiation Research Center, Hsinchu, Taiwan. All of the GISAXS data were obtained using an area detector

* Electrochemical Society Active Member.
z E-mail: jimleu@mail.nctu.edu.tw

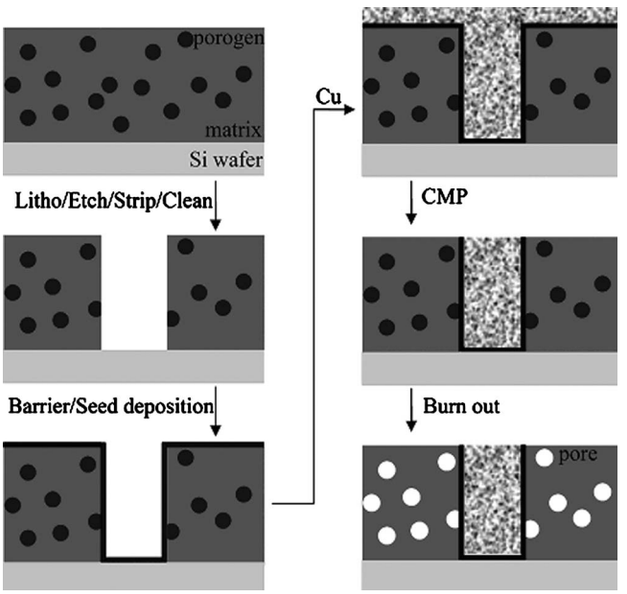

Figure 1. Schematic diagrams of damascene processing steps based on a postintegration porogen removal scheme.

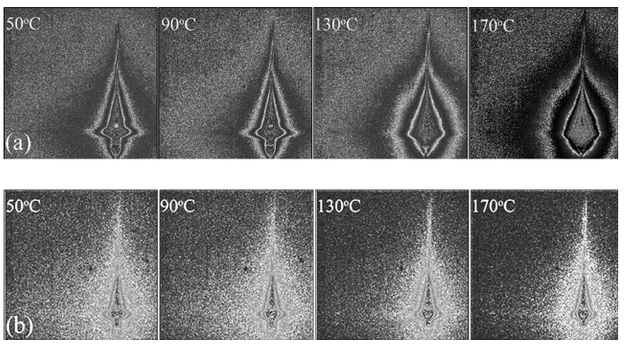

Figure 2. 2D GISAXS scattering patterns of the hybrid low-*k* films as a function of cure temperature under (a) slow curing and (b) rapid curing conditions.

that covered a q range from 0.01 to 0.1 $Å^{-1}$, and the incident angle of the X-ray beam (0.5 mm diameter) was fixed at 0.2° with an X-ray energy of 10 keV. Then, the pore size was analyzed by sphere model fitting and Guinier's law.[17-23]

The interaction between MSQ and SBS was examined by an in situ viscosity measurement using ARES (Rheometric Scientific). The viscosity data were collected from room temperature to 200°C (1) at a slow curing rate (2°C/min), and (2) isothermally at 200°C. The structural change and the degree of cross-linking of MSQ in the MSQ/porogen hybrid films were investigated as a function of temperature ranging from 25 to 200°C by FTIR spectroscopy using a Magna-IR 460 (Nicolet, Inc.) in a transmission mode with 64 scans at a spectral resolution of 2 cm^{-1}.

The elastic modulus (E) of the hybrid film was measured using a nanoindenter (MTS, Nano Indenter XP system) with a Berkovich tip. The samples were cured up to 200°C following two different curing profiles to form hybrid low-*k* films. In the slow curing method, the sample was cured in a quartz tube furnace under N_2 at a curing rate of 2°C/min to 200°C for 30 min. In the rapid curing method, the samples were cured for 30 min directly on the hot plate preheated at 200°C. The nominal film thickness of hybrid films for nanoindentation is 1200 nm, while the indentation depth is kept at 100 nm.

Results and Discussion

The porogen size of the hybrid low-*k* films before burning out were first characterized by in situ GISAXS. Figures 2a and 2b show the 2D GISAXS scattering patterns of the hybrid low-*k* films for various curing temperatures (50–210°C) at two different curing rates. In Fig. 2a, the scattering patterns of the hybrid low-*k* film cured at a slow curing rate showed significant transition between 90 and 170°C. In contrast, the scattering patterns of the low-*k* films cured at a rapid curing rate exhibited little variation, as illustrated in Fig. 2b. These scattering patterns indicate that the SBS porogens showed much diffusion and aggregation activity within the MSQ matrix when the hybrid film was cured at a slow curing rate. In contrast, the diffusion and aggregation of SBS within the MSQ matrix is very limited when the hybrid low-*k* film was cured at a rapid rate.

From GISAXS scattering patterns, the porogen sizes in the MSQ/SBS films cured under different rates at temperatures between 50 and 210°C can be further determined. In this paper, a particulate system[18] was used to analyze the scattering data by treating the pores in the matrix the same as the particles in the hybrid film. When the particle concentration is low, the scattering of the pores in the matrix does not mutually interact. Accordingly, the scattering intensity of individual particle, $I(q)$, could be defined by Eq. 1

$$I(q) = n_p(\rho_p - \rho_m)^2 V_p^2 P(q) S(q) \quad [1]$$

where the wave vector $q = 4\pi\lambda^{-1} \sin\theta$ is defined by the wavelength λ and the scattering angle 2θ of X rays, n_p is the number density of particles, ρ_p and ρ_m are the scattering density of the particle and the matrix, respectively, V_p denotes the volume of the particle, $P(q)$ is a form factor, and $S(q)$ is a structure factor. The structure factor $S(q)$ is close to 1 in a low-concentration system and thus can be ignored. Therefore, the scattering profile of $I(q)$ is only related to the form factor $P(q)$ of the particles. As a result, $I(q)$ can be furthered to the Guinier's expression,[19-21] involving radius of gyration R_g as described by Eq. 2

$$I(q) = n_p(\rho_p - \rho_m)^2 V_p^2 \exp\left(\frac{-q^2 R_g^2}{3}\right) \quad [2]$$

In this case, a linear relationship exists between $\ln(I)$ and q^2, with a slope of $(-R_g^2/3)$. Figures 3a and 3b show the $\ln(I)$ plot against q^2 in the 2D GISAXS scattering patterns of the hybrid low-*k* films cured at various temperatures under slow curing and rapid curing conditions, respectively. The slope, i.e., R_g size, showed that the porogen R_g size increased nonlinearly with the curing temperature between 50 and 210°C in the slowly cured system as shown in Fig. 3a, but varied little with temperatures between 50 and 210°C in the rapidly cured system, as shown in Fig. 3b. Since the shape of the SBS porogen in the hybrid film is close to a sphere as confirmed by a scanning electron microscope, the pore size d could be deduced from $d = 2(5/3)^{1/2} R_g$.[22,23] In addition, the porogen size distribution is estimated from the change of the slopes in the low-q region; for instance, monodispersity corresponds to a single slope. As a result, the calculated porogen size and distribution of the hybrid low-*k* films as a function of curing temperatures under slow curing and rapid curing conditions are shown in Fig. 4. Upon slow curing to 210°C, as shown in Fig. 4a, the porogen size/distribution increased from 12.7 ± 2.3 nm to 32.8 ± 5.4 nm. Moreover, the increased rate of pore size became noticeable at $T > 110$°C, and more significant between 130 and 170°C (from 17.5 ± 2.9 nm to 31.2 ± 4.9 nm), but showed little variation between 170 and 210°C (from 31.2 ± 4.9 nm to 32.8 ± 5.4 nm). In con-

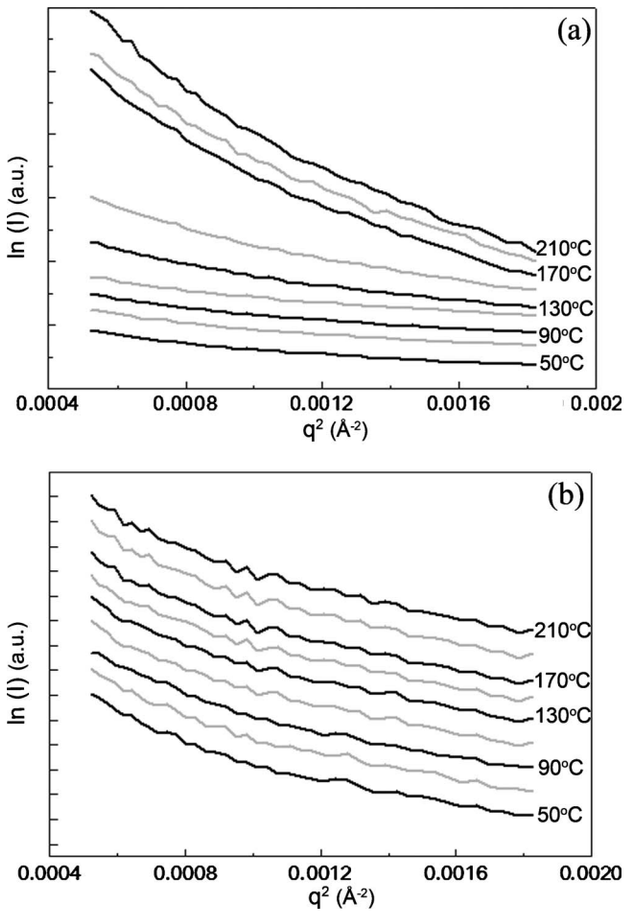

Figure 3. $\ln(I)$-q^2 plots along q_{xy} from 2D GISAXS scattering patterns of the hybrid low-*k* films cured at various temperatures under (a) slow and (b) rapid curing conditions.

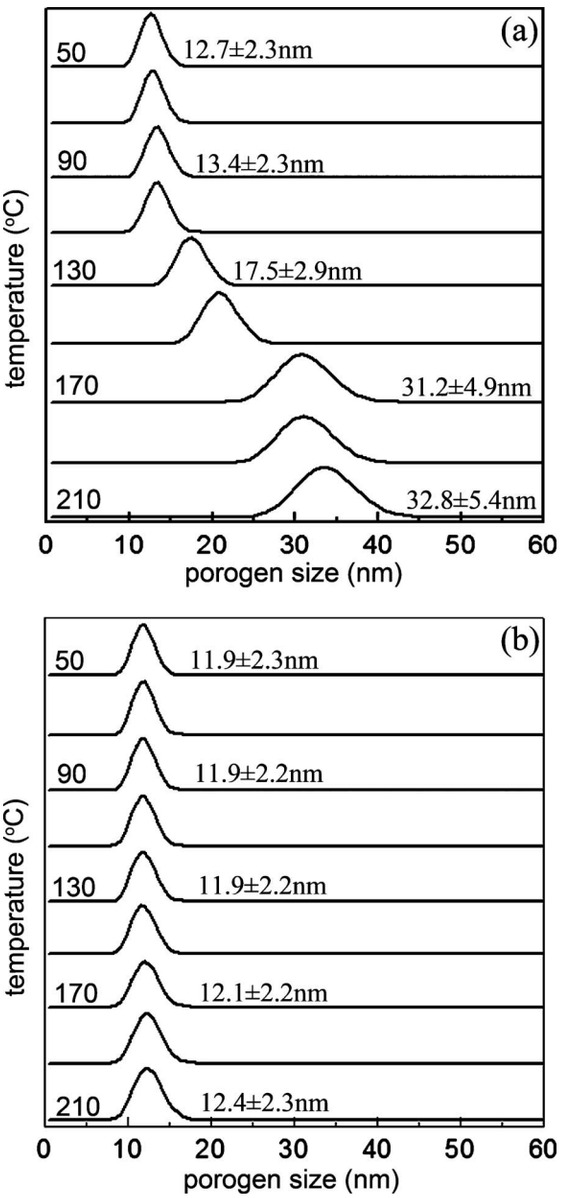

Figure 4. Porogen sizes in the hybrid low-*k* films as a function of cure temperature under (a) slow and (b) rapid curing conditions.

trast, the porogen size/distribution remained about 12 ± 2 nm with a narrow size distribution upon rapid curing up to 210°C, as shown in Fig. 4b.

Subsequently, the interaction between the SBS porogen and the MSQ matrix was examined by an in situ viscosity measurement from room temperature to 200°C (1) at a slow curing rate (2°C/min), and (2) at a rapid curing rate, i.e., isothermally at 200°C, as shown in Figs. 5a and 5b, respectively. For the slowly cured system shown in Fig. 5a, the viscosity increased linearly up to about 3800 s or 100°C when it reached the first plateau. In this period, the viscosity was strongly influenced by the solvent, i.e., THF, whose boiling point is 66°C. At this time, the molecular chains of MSQ and porogen hardly diffused and aggregated because the hybrid films behaved like a solid as the solvent, THF, was slowly evaporated, leading to film shrinkage and an increase of viscosity.[24]

Beyond 100°C, the viscosity initially remained around 210,000–230,000 poise in the plateau, then dropped drastically to 130,000 poise above 160°C and up to 170°C, and subsequently increased again up to ~250,000 poise at 200°C. In the plateau stage (100 to 160°C), the glass transition temperature (T_g) of the hybrid film played an important role on the viscosity. For the low-*k* matrix MSQ, it has a T_g around 88–111°C depending on the ratio of hydroxyl and methoxy groups within the precursor.[25] In contrast, the porogen SBS has a T_g around 98–105°C depending on the weight percentage of polystyrene and polybutadiene.[26] Based on differential scanning calorimetry measurement, the T_g's of SBS and MSQ in this study were 90 and 100°C, respectively. As the temperature exceeded 100°C, i.e., T_g of MSQ, the molecular chains of the MSQ matrix became relaxed or "rubberlike," which further enhanced the mobility of the SBS particles, resulting in a slight reduction of viscosity to ~210,000 poise. It is believed that SBS particles aggregated readily as facilitated by the rubberlike MSQ matrix at $T \geqslant T_g$.

As the temperature was increased to about 160°C, the drastic drop of viscosity in the MSQ/SBS hybrid film was presumably caused by the plasticization of H_2O released at the onset of the significant MSQ cross-linking reaction, which will be further elucidated by FTIR analysis in the following section. After 170°C, the viscosity resumed its increasing trend up to 200°C as H_2O was evaporated rapidly while the cross-linking of the low-*k* MSQ matrix continued. As a result, significant aggregation of the SBS porogen occurred during the 160–170°C stage due to its high mobility in a much reduced viscosity condition. This explained the rapid increase of porogen size and distribution at temperatures between 150 and 170°C; then the porogen size leveled off due to the limited mobility

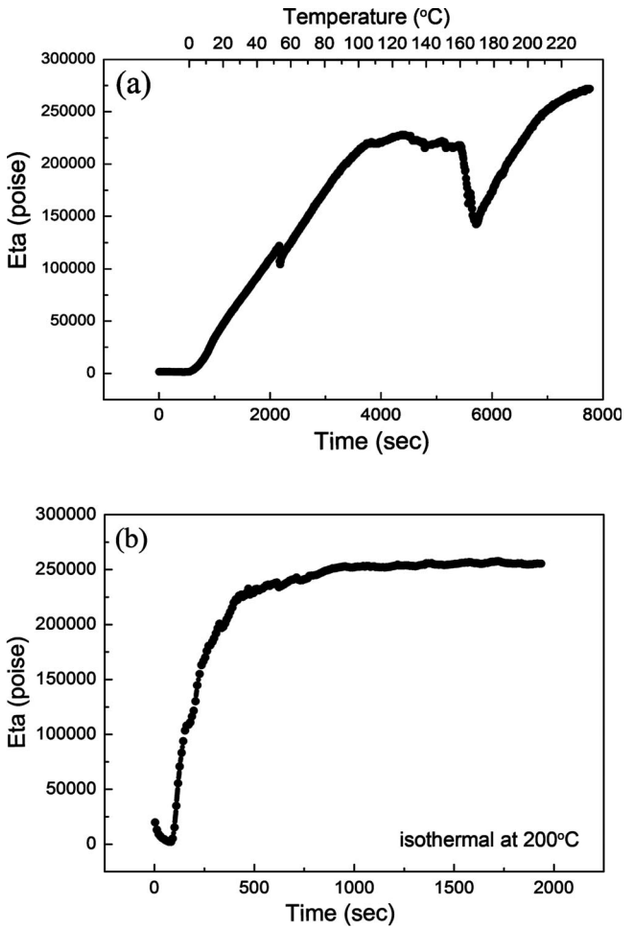

Figure 5. Viscosity of the hybrid low-*k* films as a function of cure temperature under (a) slow curing profile at 2°C/min to 250°C and (b) isothermal at 200°C.

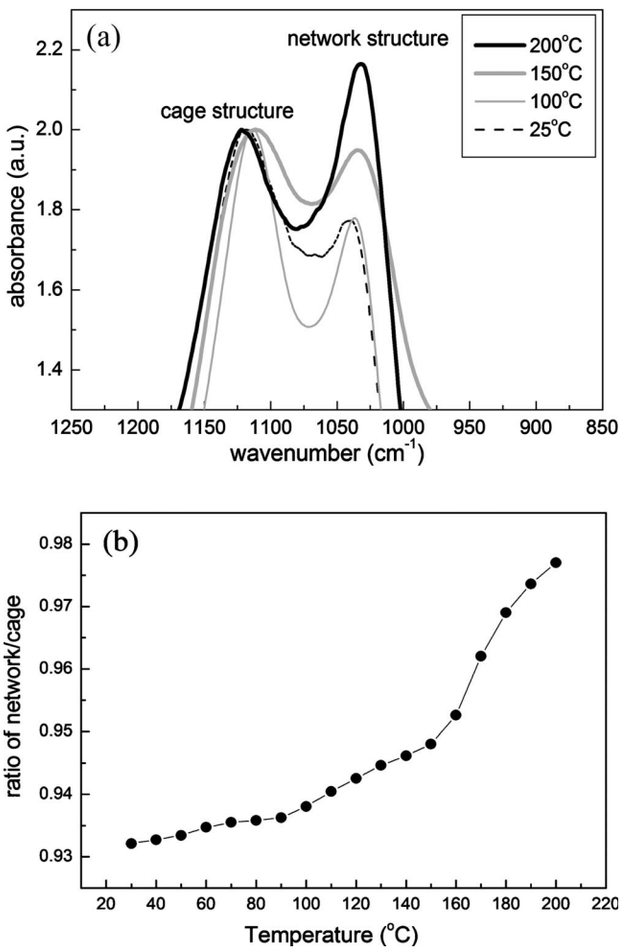

Figure 6. (a) IR spectra of MSQ/SBS hybrid films cured up to various temperatures: 25, 100, 150, and 200°C. (b) The ratio of network/cage structure in the MSQ/SBS hybrid films as a function of cure temperatures between 30 and 200°C at an interval of 10°C.

of the SBS porogen as the viscosity increased beyond 170°C. On the other hand, Fig. 5b shows the in situ viscosity of the hybrid film cured rapidly at 200°C. In this system, the viscosity rapidly reached a plateau of ~250,000 poise at 400 s. This suggested that the low-*k* MSQ matrix became very dense and rigid in a short period, inducing enormous viscosity in the film and preventing any aggregation of porogen. Thus, the size of the porogen was confined to ~12 nm with tight distribution immediately upon fast cure.

It becomes clear that the structure state of the low-*k* MSQ matrix at $T \geqslant T_g$ during the cure step plays a critical role on the viscosity of the hybrid film and porogen size. As a result, FTIR was employed to examine the structure state of the MSQ matrix in the MSQ/porogen hybrid films as a function of cure temperature. Figure 6a shows FTIR spectra of the hybrid films cured up to various temperatures such as 25, 100, 150, and 200°C. Two peaks at 1130 and 1030 cm^{-1} were attributed to Si–O stretching in the cage and network structures, respectively.[15] In addition, all IR spectra were normalized to the intensity of cage Si–O stretching at 1130 cm^{-1} and the ratio of specific absorption band to the cage Si–O absorption band was defined by its peak intensity to that of the cage Si–O band in this study for simplicity. The absorption intensity at 1030 cm^{-1} associated with the stretching of network Si–O changed slightly between 25 and 100°C based on the band broadening even though the peak height remained the same, but its intensity increased significantly when the curing temperature was raised above 100°C. To carefully examine the change rate of structural transformation from cage Si–O to network Si–O structure, the ratio of the network/cage structure in the MSQ/SBS hybrid films is shown in Fig. 6b for slow cure profile from 30 to 200°C at an interval of 10°C. The ratio increased gradually from 0.932 to 0.938 when the cure temperature was raised from 30 to 100°C. Afterwards, the ratio rose up from 0.938 at 100°C to 0.952 at 160°C, due to the condensation of silanol (Si–OH) groups in the MSQ precursor.[27] Yet, at *T* between 160 and 170°C, there was a faster increase in the ratio of the network/cage structure (from 0.952 to 0.962) as evidenced by the change of slope shown in Fig. 6b. This indicated that MSQ underwent extensive structural transformation from cage Si–O to network Si–O structure through the cleaving of the Si–O–Si group in the cage structure and condensation reaction, i.e., cross-linking with a by-product of H_2O.[27] For a short duration, the released H_2O can serve as a plasticizer in the MSQ/SBS hybrid film, reducing its viscosity between 160 and 170°C as shown in Fig. 5a. From 170 to 200°C, the ratio of network/cage structure increased at a slightly lower rate from ~0.96 up to 0.98 as the transformation to a rigid, 3D network structure continued. Continued cross-linking of the MSQ matrix in conjunction with the fast evaporation of H_2O accounted for the increasing viscosity above 170°C in Fig. 5a.

Summarizing the results of in situ viscosity measurement, the structural variation of the MSQ matrix by FTIR analysis, and porogen size by GISAXS as a function of temperature in Fig. 7, the

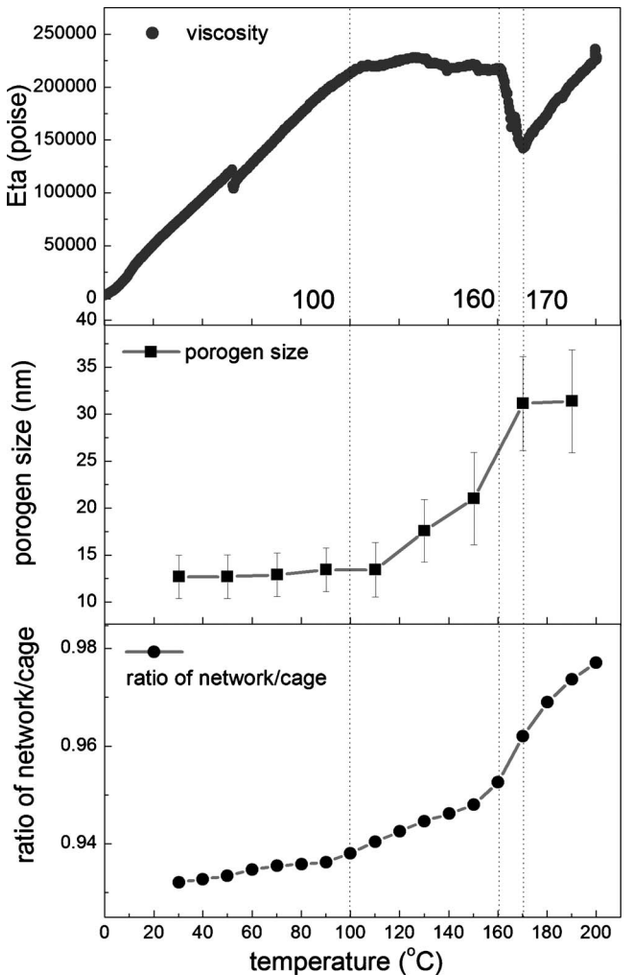

Figure 7. The viscosity, porogen size, and network/cage structure ratio of the MSQ/SBS hybrid films as a function of temperature during slow curing.

effect of the MSQ structure during the thermal cure process on the porogen aggregation behavior and its correlation with porogen size can be described and elucidated below.

For the as-spun MSQ/SBS hybrid films in this paper, the SBS porogen (5 wt %) could be considered as nanoparticles in the MSQ matrix, whose structure could change from a precursor at room temperature to a lightly cross-linked or even highly cross-linked structure depending on the cure temperature and cure rate. In turn, the structure of the MSQ matrix during the thermal cure process affected the porogen aggregation behavior and the porogen size in the MSQ/SBS hybrid films. According to the in situ viscosity measurement, porogen size measurement by GISAXS, and FTIR analysis summarized in Fig. 7, the interaction between the SBS porogen particles and the MSQ matrix for the slow cure profile could be divided into four stages; namely, (1) below 100°C, (2) 100 to 160°C, (3) 160 to 170°C, and (4) above 170°C up to 200°C. This highlights three critical temperatures: (1) glass transition temperature, T_g (~ 100°C), (2) onset temperature of network Si–O transformation (170°C), and (3) immobilization temperature (160°C), which controlled the microstructure of the MSQ matrix and, in turn, the porogen segregation and porogen size during the thermal cure process.

For temperatures below 100°C in the slow cure system, SBS porogen particles hardly diffused and aggregated within the MSQ matrix because the hybrid films behaved as a solid when THF solvent was slowly evaporated, leading to film shrinkage and an increase of viscosity. Little variation of the SBS porogen size (~ 12–13 nm) was found in this stage.

In the second stage (100 to 160°C), the MSQ matrix exhibited a low degree of cross-linking via the condensation of Si–OH groups as evidenced by the ratio of network/cage structure shown in Fig. 7, even though MSQ cross-linking started at room temperature.[28] At $T > T_g$ of the MSQ matrix, SBS possessed high mobility in the MSQ matrix, whose molecule chains fully relaxed, reducing the viscosity of the hybrid film as illustrated by Fig. 7. Therefore, the behavior of the SBS particle could be described by the kinetic molecular theory of Brownian motion based on Einstein-Stokes Eq. 3 (Refs. 29 and 30)

$$D = \frac{k_B T}{6\pi\eta r} \quad [3]$$

where k_B is the Boltzmann constant, T is the absolute temperature, η is the viscosity of the system, and r is the particle radius. At this stage, the SBS particle aggregation depended on its diffusivity, which increased with (1) increasing temperature due to higher collision frequency and (2) reduced viscosity, η, which is a measure of the steric barrier for the SBS particle to move within the MSQ matrix. Thus, the relaxation of the SBS and MSQ molecular chains at $T > T_g$ led to reduced viscosity and higher diffusivity of the SBS particles. Such high diffusivity enhanced SBS collision and led to the aggregation of SBS porogen from 13 to 22 nm.

At $T > 160$°C, the cross-linking of the MSQ precursor continued. But, we observed a noticeable transformation of the MSQ matrix from a loose cage Si–O structure to a dense network Si–O structure which served as a 3D steric barrier to the migration of the SBS particles within the MSQ matrix. One expected the viscosity of the hybrid films to increase from 170 to 200°C as a higher degree of cross-linking took place and more network Si–O structure was formed. Instead, the viscosity dropped drastically to 130,000 poise in the third stage (160 to 170°C). It is believed that when extensive transformation of cage to network Si–O occurred at $T > 160$°C, a large amount of H_2O by-products could serve as a plasticizer in the MSQ/SBS hybrid film and result in a significant reduction of viscosity. Furthermore, this enhanced the aggregation of SBS porogens resulting in a faster change of porogen size from 22 to 31 nm between 150 and 170°C.

In the final stage (170 to 200°C), most H_2O is believed to be dried up prior to 170°C. In addition, the cross-linking of the MSQ matrix with a 3D and highly cross-linked Si–O network structure at $T > 170$°C made the MSQ/CBS hybrid like a solid with very high viscosity, ~250,000 poise. Thus, SBS porogens were trapped or "frozen" within the highly cross-linked MSQ matrix, leading to an approximately constant porogen size (~ 31–32 nm) beyond $T > 170$°C. This also accounted for the small porogen size and tight distribution (12 ± 2 nm) in the MSQ/porogen hybrid films cured rapidly at 200°C/min.

The elastic moduli of the hybrid films cured under slow and fast profiles measured by the nanoindentation method were 4.9 and 5.6 GPa, respectively. For the same degree of MSQ cross-linking, their difference in the modulus was caused by the different porogen sizes.[31] Based on an in situ GISAXS measurement for the hybrid film cured in the slow curing step, the porogen aggregated and formed an interconnected mass in the matrix with sizes up to 33 nm, reducing the mechanical strength of the hybrid film. In contrast, the hybrid film cured rapidly possessed higher strength due to a smaller porogen size (~12 nm) trapped within a highly cross-linked MSQ matrix. Thus, the rapid curing method makes the MSQ/high-temperature porogen hybrid films strong in mechanical property with small porogen size and practical for the postintegration porogen removal scheme. In addition, the rapid curing method has been widely adapted in the industry to shorten the processing time and reduce cost.[32,33] The low-k films are typically prepared using a soft bake on the hot plate to remove the solvent, then cured or hard

baked at a higher temperature in the furnace to burn out the porogen. Based on the results of this paper, we recommend that the soft-bake temperature is kept below the glass transition temperature of the porogen when the rapid curing method is used. On the other hand, the hard-bake temperature should be kept at least higher than the immobilization temperature of the low-k matrix, which is $>170°C$ for the MSQ matrix in this paper.

Conclusion

A commercial, spin-on organosilicate, i.e., MSQ was selected as the low-k matrix and a high-temperature porogen, such as SBS, was employed as the sacrificial component in this paper. The effect of the MSQ structures under different thermal cure profiles (slow, 2°C/min vs rapid, 200°C/min) on the porogen aggregation behavior and its size in the hybrid MSQ/SBS films cured up to 200°C were investigated by in situ GISAXS, viscosity measurement, and FTIR analysis. For slow curing, significant porogen diffusion and aggregation occurred between 100 and 200°C, at which the porogen size increased from 12 to 34 nm. The aggregation of SBS in the hybrid MSQ/SBS films was greatly influenced by the structural state of the MSQ matrix at three controlling temperatures; namely, (1) glass transition temperature, T_g (100°C), (2) onset temperature (160°C) for transforming Si–O cage Si–O to network Si–O structure, and (3) immobilization temperature (170°C). The porogen size started growing as SBS porogen aggregated at $T > T_g$ of MSQ, then increased at a higher rate at $T > 160°C$ as the viscosity drastically dropped down to ~130,000 poise due to the plasticization of a vast amount of H_2O released by the condensation reaction involving the transformation of cage Si–O to network Si–O structure, and finally remained about constant at ~32 nm after 170°C, at which the MSQ matrix was highly cross-linked to immobilize SBS particles. In contrast, upon rapid curing, the SBS porogen was trapped within a rapidly formed, well-cross-linked MSQ matrix, leaving its size unchanged at approximately 12 nm with tight distribution. Furthermore, the elastic modulus of the hybrid film cured rapidly possessed higher strength due to the smaller porogen size. Thus, the rapid curing method makes the MSQ/high-temperature porogen hybrid films strong in mechanical property with small porogen size and practical for the postintegration porogen removal scheme. In summary, this paper elucidates the interaction mechanism between porogen and the MSQ matrix and its correlation with porogen size. In addition, we provide a methodology for controlling the porogen size by adjusting the curing profile in terms of cure temperature and rate.

Acknowledgments

The authors thank Kuo-Yuan Hsu for viscosity rheometer tests and Dr. Chiu-Hun Su and Kuei Fen Liao for their assistance in the GISAXS measurements. This work was financially supported by National Science Council of Taiwan through contract no. NSC 98-2221-E009-177 and no. NSC 99-2221-E009-177.

National Chiao Tung University assisted in meeting the publication costs of this article.

References

1. M. T. Bohr, *Solid State Technol.*, **9**, 4 (1996).
2. P. W. Lee, S. Mizuno, A. Verma, H. Tran, and B. Nguyen, *J. Electrochem. Soc.*, **143**, 2015 (1996).
3. S. Yang, P. A. Mirau, C. D. Pai, O. Nalamasu, E. Reichmanis, E. K. Lin, H. J. Lee, D. W. Gidley, and J. Sun, *Chem. Mater.*, **13**, 2762 (2001).
4. M. Fayolle, G. Psaaemard, O. Louveau, F. Fusalba, and J. Cluzel, *Microelectron. Eng.*, **70**, 255 (2003).
5. M. Ree, J. Yoon, and K. Heo, *J. Mater. Chem.*, **16**, 685 (2005).
6. A. M. Padovani, L. Rhodes, S. A. B. Allen, and P. A. Kohl, *J. Electrochem. Soc.*, **149**, F161 (2002).
7. S. Baskaran, J. Liu, K. Dormansky, N. Kohler, X. Li, C. Coyle, G. E. Fryxell, S. Thevuthasan, and R. E. Williford, *Adv. Mater.*, **12**, 291 (2002).
8. T. Yamada, H. Zhou, K. Asai, and I. Honma, *Mater. Lett.*, **56**, 93 (2002).
9. S. Yang, P. A. Mirau, C. Pai, O. Nalamasu, E. Reichmanis, J. C. Pai, Y. S. Obeng, J. Seputro, E. K. Lin, H. Lee, et al., *Chem. Mater.*, **14**, 369 (2002).
10. H. C. Kim, J. B. Wilds, C. R. Kreller, W. Volksen, P. J. Brock, V. Y. Lee, T. Magbitang, J. L. Hedrick, C. J. Hawker, and R. D. Miller, *Adv. Mater.*, **14**, 1637 (2002).
11. Q. R. Huang, W. Volksen, E. Huang, M. Toney, C. W. Frank, and R. D. Miller, *Chem. Mater.*, **14**, 3676 (2002).
12. J. N. Sun, Y. Hu, W. E. Frieze, W. Chen, and D. W. Gidley, *J. Electrochem. Soc.*, **150**, F97 (2003).
13. K. Mosig, T. Jacobs, K. Brennan, M. Rasco, J. Wolfe, and R. Augur, *Microelectron. Eng.*, **64**, 11 (2002).
14. J. Calvert and M. Gallagher, *Semicond. Int.*, **26**, 52 (2003).
15. W. C. Liu, C. C. Yang, W. C. Chen, B. T. Dai, and M. S. Tsai, *J. Non-Cryst. Solids*, **311**, 233 (2002).
16. A. Zenasni, F. Ciaramella, V. Jousseaume, C. L. Cornec, and G. Passemard, *J. Electrochem. Soc.*, **154**, G6 (2007).
17. Y. H. Lai, Y. S. Sun, U. Jeng, J. M. Lin, T. L. Lin, H. S. Sheu, W. T. Chuang, Y. S. Huang, C. H. Hsu, M. T. Lee, et al., *J. Appl. Crystallogr.*, **39**, 871 (2006).
18. R. J. Roe, *Methods of X-Ray and Neutron Scattering in Polymer Science*, Chap. 5, Oxford University Press, New York (2000).
19. A. Guinier, *Ann. Phys.*, **12**, 161 (1939).
20. D. J. Kinning and E. L. Thomas, *Macromolecules*, **17**, 1712 (1984).
21. J. S. Pedersen, *J. Appl. Crystallogr.*, **27**, 595 (1994).
22. L. A. Feigin and D. I. Svergun, *Structure Analysis by Small Angle X-ray and Neutron Scattering*, Plenum, New York (1987).
23. A. Guinier and G. Fournet, *Small-Angle Scattering of X-rays*, John Wiley & Sons, New York (1955).
24. J. Fuwukawa, *Polym. Bull. (Berlin)*, **10**, 336 (1983).
25. Q. R. Huang, H.-C. Kim, E. Huang, D. Mecerreyes, J. L. Hedrick, W. Volksen, C. W. Frank, and R. D. Miller, *Macromolecules*, **36**, 7661 (2003).
26. R. J. Young and P. A. Lovell, *Introduction to Polymers*, Chapman & Hall, London (1991).
27. H. W. Ro, E. S. Park, C. L. Soles, and D. Y. Yoon, *Chem. Mater.*, **22**, 1330 (2010).
28. C. Y. Wang, Z. X. Shen, and J. Z. Zheng, *Appl. Spectrosc.*, **54**, 209 (2000).
29. N. Wiener, *J. Math. Phys.*, **2**, 131 (1923).
30. H. T. Healy and Y. C. Zhang, *Phys. Rep.*, **254**, 215 (1995).
31. G. Ouyang, G. Yang, C. Sun, and W. Zhu, *Small*, **4**, 1359 (2008).
32. T. Yamazaki, M. Hirakawa, T. Nakayama, and H. Murakami, in *IEEE Proceedings of the International Interconnect Technical Conference*, IEEE, p. 119 (2009).
33. T. Kokubo, A. Das, Y. Furukawa, I. Vos, F. Iacopi, H. Struyf, J. V. Aelst, M. Maenhoudt, Z. Tokei, I. Vervoort, et al., in *IEEE Proceedings of the International Interconnect Technical Conference*, IEEE, p. 51 (2002).